AIP Journal of Applied Physics

Filtered pulsed cathodic arc deposition of fullerene-like carbon and carbon nitride films

Mark D. Tucker, Zsolt Czigány, Esteban Broitman, Lars-Åke Näslund, Lars Hultman, and Johanna Rosen

Citation: Journal of Applied Physics **115**, 144312 (2014); doi: 10.1063/1.4871179
View online: http://dx.doi.org/10.1063/1.4871179
View Table of Contents: http://scitation.aip.org/content/aip/journal/jap/115/14?ver=pdfcov
Published by the AIP Publishing

Filtered pulsed cathodic arc deposition of fullerene-like carbon and carbon nitride films

Mark D. Tucker,[1,a)] Zsolt Czigány,[2] Esteban Broitman,[1] Lars-Åke Näslund,[1] Lars Hultman,[1] and Johanna Rosen[1]
[1]*Thin Film Physics Division, Department of Physics, Chemistry and Biology (IFM), Linköping University, SE-58183 Linköping, Sweden*
[2]*Institute for Technical Physics and Materials Science, RCNS, Hungarian Academy of Sciences, P.O. Box 49, H-1525 Budapest, Hungary*

(Received 24 January 2014; accepted 25 March 2014; published online 14 April 2014)

Carbon and carbon nitride films (CN_x, $0 \le x \le 0.26$) were deposited by filtered pulsed cathodic arc and were investigated using transmission electron microscopy and X-ray photoelectron spectroscopy. A "fullerene-like" (FL) structure of ordered graphitic planes, similar to that of magnetron sputtered FL-CN_x films, was observed in films deposited at 175 °C and above, with N_2 pressures of 0 and 0.5 mTorr. Higher substrate temperatures and significant nitrogen incorporation are required to produce similar FL structure by sputtering, which may, at least in part, be explained by the high ion charge states and ion energies characteristic of arc deposition. A gradual transition from majority sp^3-hybridized films to sp^2 films was observed with increasing substrate temperature. High elastic recovery, an attractive characteristic mechanical property of FL-CN_x films, is evident in arc-deposited films both with and without nitrogen content, and both with and without FL structure.
 [http://dx.doi.org/10.1063/1.4871179]

I. INTRODUCTION

"Fullerene-like" carbon nitride films, FL-CN_x, consist of graphitic basal planes that are curved and cross-linked as a consequence of the substitutional bonding of nitrogen within the plane.[1,2] Extensive experimental work into these materials, synthesized by reactive magnetron sputter deposition, has shown that this interlinked structure results in films with unusual and useful mechanical properties. Notably, FL-CN_x coatings can have extremely high elasticity, evidenced by high elastic recovery after nanoindentation.

C-N films have also been produced by arc evaporation using a variety of DC and pulsed-arc processes, and by pulsed laser deposition,[3–5] in addition to magnetron sputtering. Early experiments were often attempts to produce the C_3N_4 phase predicted by Liu and Cohen, or to modify the electronic properties of tetrahedral amorphous carbon (ta-C). This work demonstrated that arc-deposited ta-C could incorporate a few percent of nitrogen, while retaining a similar structure to undoped ta-C.[3] At higher N_2 concentrations, no sp^3-bonded carbon is observed. The maximum nitrogen concentration found varies from around 25 at. %[3,6] to 34 at. %.[7] Similar results are obtained with pulsed laser deposition.[8]

The structure of arc-deposited CN_x, as revealed by transmission electron microscopy (TEM), has not been investigated as a function of deposition parameters to the same extent as sputter-deposited FL-CN_x. Some intriguing results have been published showing fullerene-like structure in laser-triggered arc deposited carbon films,[9] but for the most part, studies of arc-deposited CN_x have focused on characterisation through electron scattering and Raman spectroscopy. We have deposited carbon and carbon nitride films by pulsed cathodic arc deposition, and we consider the microstructure of these coatings in relation to the well-characterized sputtered FL-CN_x materials, using TEM and X-ray photoelectron spectroscopy (XPS) characterization and varying the deposition parameters of substrate temperature and nitrogen pressure. We then compare the processes known to lead to the formation of FL-CN_x by sputter deposition with the processes occurring during deposition of carbon nitride by pulsed cathodic arc.

II. EXPERIMENTAL METHODS

A pulsed, filtered cathodic arc deposition system was used to deposit C and CN_x films. A system of similar design is described by Ryves *et al.*[10] In this system, a high current arc discharge is repeatedly ignited on a 25 mm diameter cathode by surface flashover between the cathode and a centre trigger electrode, and the arc plasma generated is transported through a 90° magnetic filter to the substrate. The filter is a solenoid of 30 turns, with a diameter of 0.15 m. The path length from the cathode to the substrate through the solenoid is 0.6 m. A pulsed current is applied through the filter solenoid in synchronisation with the arc current pulses. The average filter current during the arc pulse was 0.5 kA for these experiments. The chamber base pressure is $\sim 1 \times 10^{-6}$ Torr ($\sim 1 \times 10^{-4}$ Pa). For reactive deposition, N_2 gas is introduced into the chamber at a point away from both the substrate and the cathode at a constant mass flow rate. The chamber pressure is regulated using the signal from a capacitance manometer to control a butterfly valve throttling the chamber pumping speed.

For these experiments, the arc was operated on a graphite cathode, to which pulses of peak current 1.8 kA and

a)Electronic mail: martu@ifm.liu.se

length 0.6 ms were applied at a rate of 10 Hz. The film growth rate with these parameters was 0.083 nm/pulse, for depositions without nitrogen onto a substrate at 20 °C. In the case of reactive deposition, the growth rate decreased with increasing nitrogen pressure, falling to 0.029 nm/pulse for deposition at 20 mTorr (2.7 Pa).

Samples were deposited onto substrates of (100) silicon and freshly cleaved (100) NaCl held at a temperature T_s set between 20 and 450 °C. The substrate heater was calibrated against measurements from a thermocouple welded to a metal foil test substrate. The samples grown on Si substrates were deposited with either 500 or 5000 arc pulses, to obtain films of 42 nm and 420 nm thickness for deposition without nitrogen. The samples grown on NaCl were deposited for 120 pulses, to obtain films of ~10 nm thickness. The sample holder was electrically connected to the chamber ground for all depositions. Samples were deposited at N_2 pressures of 0.5, 1, 2, 5, 10, and 20 mTorr (0.067, 0.13, 0.27, 0.67, 1.3, 2.7 Pa) and at the chamber base pressure. Samples deposited at base pressure will be referred to as "0 mTorr" depositions although strictly they are "≤0.001 mTorr" depositions.

Film densities and thicknesses were measured using X-ray reflectometry (XRR), using a PANalytical Empyrean diffractometer equipped with a hybrid X-ray mirror and a collimator. Each sample was aligned in the ω axis for specular reflection at 1° to an accuracy of better than 0.02°. To determine the critical angle, the data were fitted with the PANalytical X'Pert Reflectivity program, using a single-layer model.

XPS measurements of the 500 pulse samples were made with Al K_α radiation using a Kratos Axis Ultra^{DLD} system, which provided XPS spectra with an overall energy resolution better than 0.5 eV determined through the full width at half maximum of the first derivative of the Fermi edge E_f of an Au reference sample. The binding energy scale of each XPS spectrum was calibrated against the Fermi edge of Au, which was set to a binding energy of 0 eV. The XPS data were collected without sputter cleaning the sample surface.

The mechanical properties of the 5000 pulse samples were measured using a Hysitron TI 950 Triboindenter nanoindentation system. A Berkovich tip was used to indent to a maximum load of 700 μN. The hardness H and the reduced Young's modulus E_r were calculated according to the method of Oliver and Pharr.[11] The penetration displacement of the indenter at maximum load h_{max} and the final displacement h_f recorded in the unloading curve were used to determine the percentage of elastic recovery % R.[12]

The films on NaCl substrates were prepared for TEM by floating the films off the substrates in water and collecting them on TEM grids. Cross sectional TEM samples were prepared by ion beam milling.[13] The ion beam milling procedure was finished with low energy Ar^+ ions at 250 eV to eliminate ion beam damage of CN_x.[14] TEM images and electron energy loss spectra (EELS) of these samples were obtained with an FEI Tecnai G2 microscope fitted with a Gatan parallel EELS spectrometer. Diffraction patterns were collected on imaging plates in a Philips CM20 microscope.

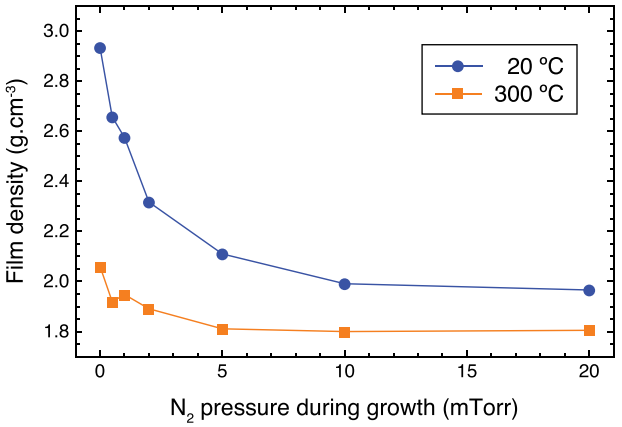

FIG. 1. The density of C and CN_x films deposited at T_s 20 or 300 °C as a function of N_2 pressure during deposition, determined by XRR.

III. RESULTS AND DISCUSSION

A. Density and composition

The density of the deposited film as a function of nitrogen pressure and substrate temperature during deposition is shown in Figure 1. The density of the 20 °C, 0 mTorr film, 2.93 g cm^{-3}, is consistent with arc-deposited ta-C with an sp^3 fraction of about 75%.[15] As the nitrogen pressure and substrate temperature increase, the film density decreases substantially, and once the nitrogen pressure reaches 10 mTorr, the film density levels out, to 2.0 g cm^{-3} at 20 °C and 1.8 g cm^{-3} at 300 °C. These densities are significantly lower than the typical ~2.5 g cm^{-3} density of CN_x films deposited by magnetron sputtering,[16] although in comparing the values it should be noted that the sputtered films' density was determined from the EELS plasmon energy and so it is a microscopic value and potentially greater than the bulk density.

The nitrogen atomic fraction, [N]/([C] + [N]), of the deposited films is shown in Figure 2. The data were calculated from XPS survey spectra using tabulated sensitivity factors. The maximum N atomic fraction reached is 0.26 at 10–20 mTorr and 20 °C. This maximum N fraction is comparable to values found in previous studies into DC- and pulsed-arc films of approximately 15–20 at. %.[3,4] Sjöström *et al.* reported a maximum N content of 25 at. % for sputtered CN_x films.[17]

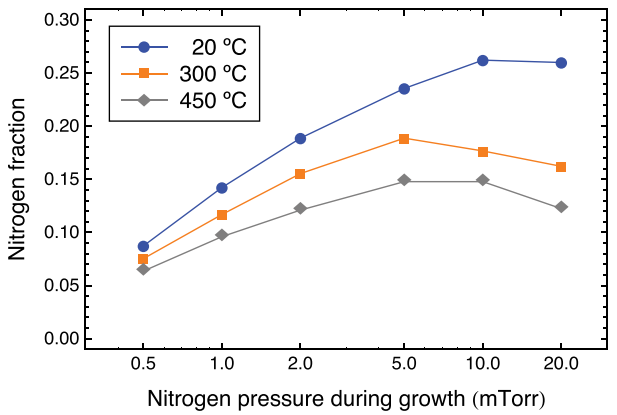

FIG. 2. The nitrogen atomic fraction of CN_x films deposited at T_s 20, 300, and 450 °C as a function of N_2 pressure, determined by XPS.

The limitation on N content in CN_x films has been attributed to a process of "chemical sputtering," where species, including N_2 and C_2N_2 form and are lost from the film.[18,19] The similarity of the maximum N fraction in our films with the maximum N fraction in sputtered CN_x films suggests that the same mechanism occurs in both cases. We observed a significant decrease in N content when the substrate temperature was increased from 20 to 300 °C (Figure 2), whereas for deposition using reactive magnetron sputtering, no decrease in N content was observed until the substrate temperature exceeded 400 °C.[17] The more energetic deposition flux in arc deposition, compared to sputter deposition,[20] is a source of additional energy at the film surface. The probability that reactions forming volatile species will occur is increased,[21,22] and so chemical sputtering occurs at lower temperatures.

B. Structure and bonding

Figure 3 shows plan view TEM images of the films deposited on NaCl substrates. The films appear homogeneous, and no porosity or voids are evident. All the samples deposited at a substrate temperature of 20 °C show the uniform speckle typical of amorphous materials. The samples deposited at 175 °C–450 °C and at 0 mTorr or 0.5 mTorr N_2 show order, with curved, parallel planes visible in the images. This appearance will be referred to as "FL" or fullerene-like structure in the following discussion. Finally, the samples deposited at 5 mTorr N_2 show an amorphous speckle pattern, with ordered planes somewhat visible in the 450 °C sample.

Figure 4 shows radial averages of electron diffraction (ED) patterns of the samples imaged in Figure 3. The ED can be used to divide the samples into three groups. The first group consists of the 20 °C samples at 0 and 0.5 mTorr. These samples show the two broad peaks at about 0.5 and 0.9 $Å^{-1}$ that are typical of ta-C, seen, for example, in DC-arc deposited ta-C (Fig. 13(g) in Ref. 23). The samples in the second and third groups show electron diffraction features associated with the lattice spacings of graphite. The peaks at approximate positions 0.3 $Å^{-1}$ and 0.6 $Å^{-1}$ correspond to the graphite (002) and (004) planes, and the peak at 0.5 $Å^{-1}$ corresponds to the graphite (100) plane.[24] In the second group of samples, those which show FL structure in TEM imaging, the (002) and (004) peaks are of high intensity. In the third group, the samples deposited at 5 mTorr, the (002) and (004) peaks are of low intensity. The diffraction patterns of the 5 mTorr samples are similar to previously reported patterns of a-C and CN_x films deposited by DC cathodic arc at high N_2 pressure.[25]

The fractions of sp^3 carbon in the 20 °C samples were 0.61 and 0.57 for deposition at 0 mTorr and 0.5 mTorr,

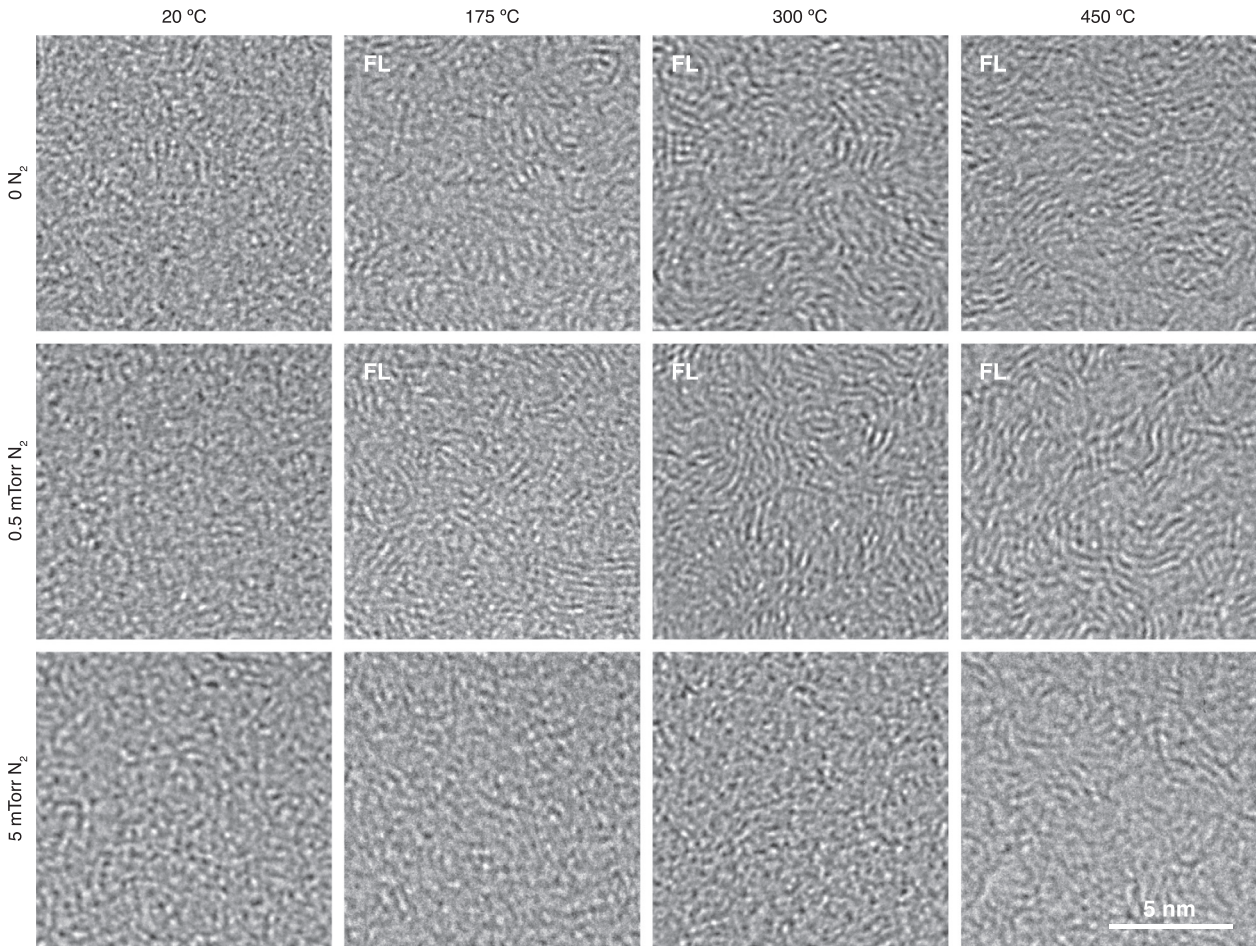

FIG. 3. Plan view TEM images of C and CN_x films deposited at T_s 20–450 °C and at N_2 pressure 0, 0.5, or 5 mTorr. Each image is at the same magnification. "FL" indicates a sample with fullerene-like appearance and a sharp electron diffraction feature corresponding to the basal plane spacing of graphite.

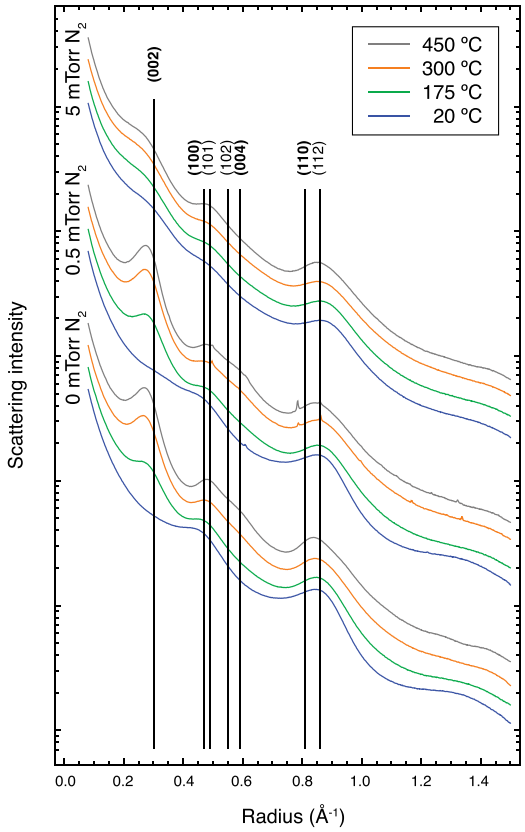

FIG. 4. Radial averages of the electron diffraction patterns of the samples shown in Figure 3. The data for each sample are offset vertically. The small spikes in some of the data are caused by remnants of the NaCl substrate. The d-spacings of some of the crystallographic planes of graphite are overlaid for comparison.

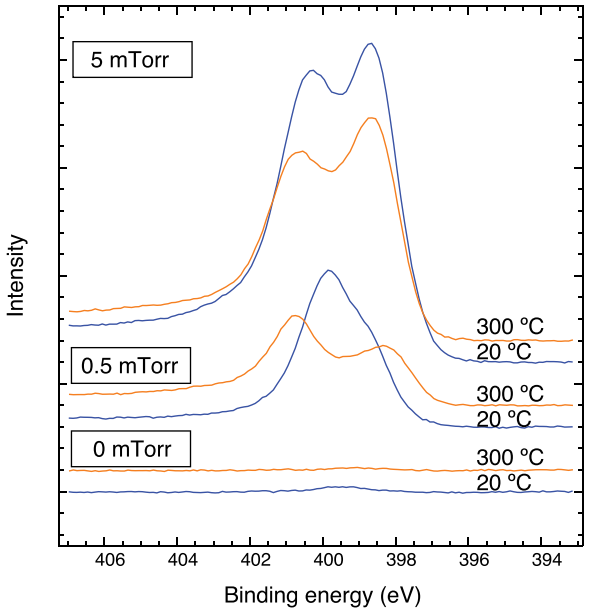

FIG. 5. XPS N(1s) edges of C and CN_x films deposited at T_s 20 or 300 °C and at N_2 pressure 0, 0.5, or 5 mTorr. The data are shown normalized to equal intensity in the pre-edge region.

respectively, determined from the carbon K edge EELS data using the procedure described by Berger.[26] These values are likely to be lower than the true sp^3 fraction of the films, as since the TEM samples were thin (~10 nm) the expected surface sp^2 layer will contribute to the EELS spectrum. C-N bonding was not considered as the atomic fraction of N in the N-containing sample was less than 10%. The 300 °C, 0 mTorr sample was used as the 100% sp^2 reference for the sp^3 fraction measurement as arc-deposited carbon films grown above about 250 °C are entirely sp^2 bonded.[27,28]

XPS N(1 s) spectra are shown in Figure 5. The N(1 s) spectra of the nitrogen-containing samples show two main peaks, at binding energies of 398–399 eV and 400–401 eV. In the analysis of CN_x film spectra, the 400 eV peak is usually associated with nitrogen bonded substitutionally in graphite, and the 398 eV peak is associated with nitrogen bonded in a "pyridine-like" configuration, i.e., at the edge of a graphite sheet.[29,30] The 398 eV peak is more prominent in less ordered films, as in these films the graphitic basal planes are smaller in extent and so a greater fraction of N is bound at their edges.

The N(1 s) spectra divide the samples into three groups in a manner consistent with the TEM and ED observations. In the first group is the 20 °C, 0.5 mTorr sample, with an N(1 s) spectrum made up of two closely spaced peaks. The EELS observations of this sample showed sp^3 bonding, and so the N(1 s) peak at 398 eV is likely to include a contribution from nitrogen bonded to sp^3-hybridised carbon, which is also a possible assignment of the 398 eV peak.[31] In the second group are the nitrogen-containing samples showing FL structure, where the N(1 s) 400 eV peak is more intense than the N(1 s) 398 eV peak. In the more ordered FL structure a greater fraction of graphitic planes is present and so more N is bonded substitutionally within the planes, increasing the intensity of the N(1 s) 400 eV peak relative to the 398 eV peak. In the third group are the samples grown at a pressure of 5 mTorr, where FL structure was not observed. In these less ordered samples, the 400 eV peak is of lower intensity than the 398 eV peak, and N bonding in the pyridine-like configuration is predominant.

XPS C(1 s) spectra are shown in Figure 6. The two major contributions to the C(1 s) spectra are a peak at 284 eV due to sp^2 carbon bonding, and a peak at 285 eV due to sp^3 bonding.[32] Additional features associated with carbon-nitrogen bonding are also visible in the 5 mTorr samples. The C(1 s) spectra of the 20 °C, 0 and 0.5 mTorr samples show a contribution at 285 eV due to sp^3 bonding, consistent with the EELS data.

The C(1 s) edge was measured on a sample set deposited at closely spaced temperature increments to investigate the nature of the C sp^3–sp^2 transition for deposition temperatures in the range 20–180 °C. The C(1 s) spectra show that the transition from sp^3 to sp^2 bonding is gradual, with some sp^3 bonding still present at 180 °C. The transition temperature and the sharpness of the transition are similar for deposition without nitrogen and for deposition with nitrogen at 0.5 mTorr. This gradual transition is confirmed by XRR measurements of the 20–180 °C sample series, shown in Figure 7, which demonstrate a gradual decrease in film density—and therefore sp^3 fraction—with increasing substrate temperature. Often, and in contrast to these results, a sharp transition between the sp^3 and sp^2 forms of arc-deposited C films is observed as the substrate temperature is increased to around

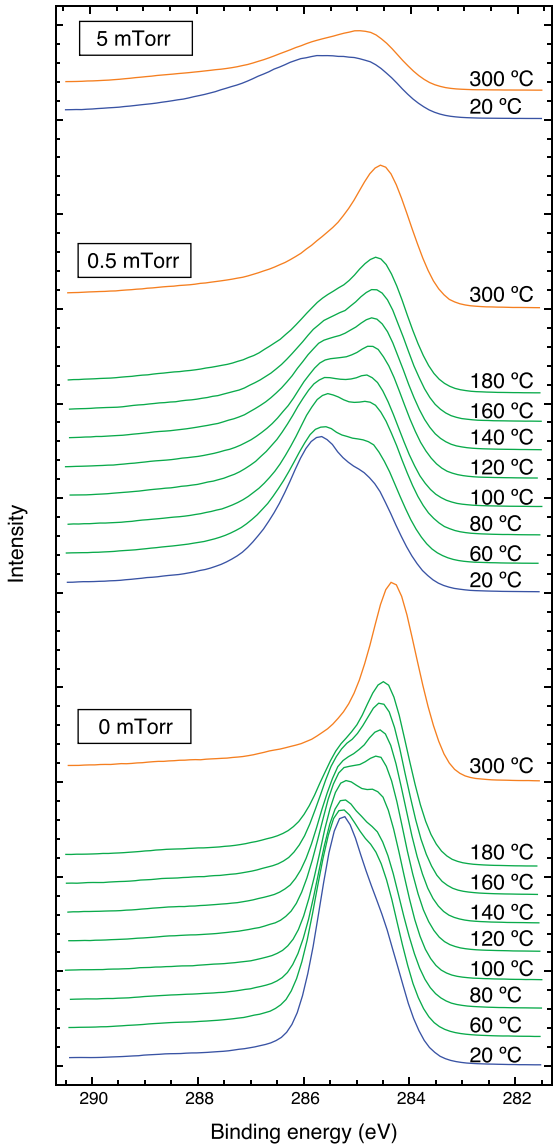

FIG. 6. XPS C(1s) edges of C and CN_x films deposited at T_s 20–300 °C and at N_2 pressure 0, 0.5, or 5 mTorr. All spectra are shown normalized to equal intensity in the pre-edge region.

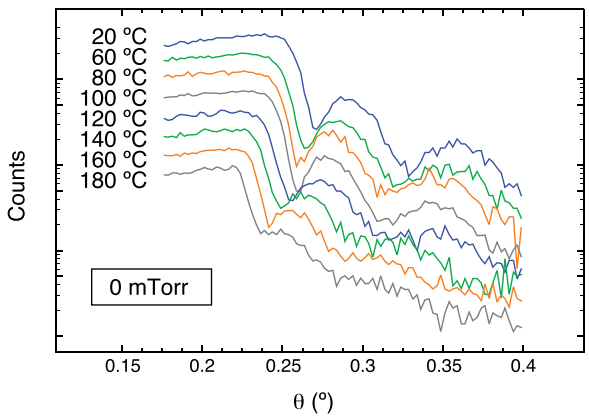

FIG. 7. XRR scans of C films deposited at T_s 20–300 °C, showing a gradual decrease in the critical angle for total reflection, and so the film density and sp^3 fraction, with increasing T_s.

200 °C.[33] A similar sharp transition is observed in experiment and in computational simulations as the energy of the deposited C ions is increased.[34] The energy threshold for the sp^3–sp^2 transition is overcome by supply of energy from energetic ions and substrate heating. Hence, our finding of a gradual transition may be explained by the wide ion energy distributions and generally higher ion energies obtained from pulsed cathodic arc depositions, in particular, in the presence of a magnetic field.[35]

C. Texture in sp^2-hybridized arc deposited C and CN_x films

The FL structure observed in the plan-view TEM imaging is consistent with both an isotropic structure of curved graphitic sheets and a structure in which the graphitic sheets are oriented parallel to the film normal. To investigate, a cross-sectional TEM sample was prepared and electron diffraction patterns of the plan-view specimens were collected with a sample tilt of 45° to the electron beam, the maximum tilt possible in the CM20 microscope.

The cross-sectional TEM image of the 300 °C, 0.5 mTorr sample, Figure 8, shows alignment of atomic planes perpendicular to the substrate, with a spacing (from the ED pattern) matching the (002) spacing of graphite. This standing basal plane texture was also evident in the tilted diffraction patterns of the plan-view specimens, where intensity variations in the diffraction rings corresponding to the graphite (002) and (004) planes appeared when the sample was tilted. Figure 9 illustrates this for the samples deposited at 0.5 mTorr N_2. The variation in intensity in the (002) and (004) features, and so the degree of texture, increases with the substrate temperature. This trend of increasing texture with substrate temperature was also observed in the samples deposited at 0 mTorr N_2. For the 5 mTorr samples, however, little change in the diffraction patterns was observed when the samples were tilted, and so the perpendicular basal-plane texture is much reduced at higher N_2 pressure.

Previous work has found a similar texture to our observations, of "standing basal planes," in sputter deposited CN_x

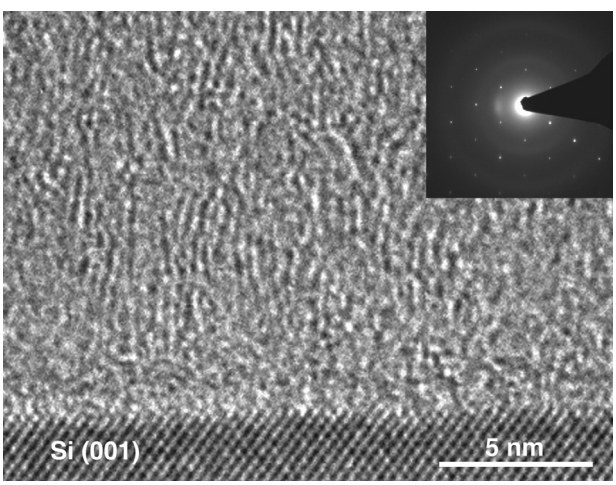

FIG. 8. A cross-sectional TEM image of a CN_x film deposited at T_s 300 °C and at N_2 pressure 0.5 mTorr, showing graphitic basal planes perpendicular to the substrate.

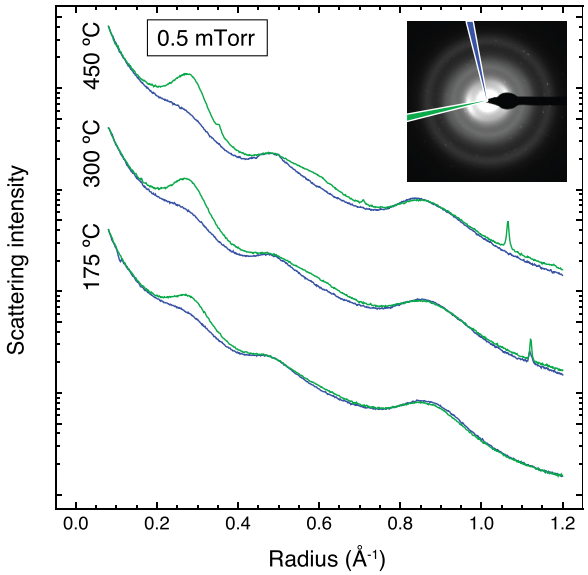

FIG. 9. Radial averages of the electron diffraction patterns of CN_x samples, collected with 45° sample tilt relative to the electron beam, showing increasing texture with increasing deposition temperature. For each diffraction pattern, a radial average was taken along a 4° sector centred on the maximum of the 0.3 $Å^{-1}$ diffraction ring, and a second radial average was taken along a sector at 90° to the maximum. The inset illustrates this for the diffraction pattern of the 450 °C sample. The small spikes in some of the data are due to substrate residue.

films.[36] This texture was observed only at higher substrate temperatures (of 350 °C or more) and at high nitrogen concentrations (of 25–30 at. % N)—the conditions required to produce films of FL structure by sputtering. In contrast, we observe the strongest standing basal plane texture in samples of lower or zero nitrogen content.

Vertical graphitic planes have been observed in DC arc deposited films grown at room temperature when the substrate bias, and so the incident C ion energy, is increased above a threshold value.[34,37] In this case, the transition is abrupt and from an sp^3 form to oriented graphitic planes, whereas our results show gradually increasing texture in parallel with gradually increasing sp^2 content as the deposition temperature is increased. As discussed above, these results may be explained by the supply of energy from the wide ion energy distribution and the generally higher ion energies obtained by pulsed cathodic arc, in particular, in the presence of a magnetic field.[35]

D. Mechanical properties

The mechanical properties measured are shown in Table I, and typical loading and unloading curves are shown in Figure 10. The hardness values measured span from 49 GPa for the 20 °C, 0 mTorr sample to 8.3 GPa for the 300 °C, 5 mTorr sample. The highest measured values are consistent with other measurements of arc-deposited ta-C. The hardness of sputtered FL-CN_x films is in the lower part of this range. The hardness and elastic modulus both decrease as the substrate temperature or the nitrogen pressure during deposition increase.

The most elastic of our films showed a recovery of 95%, a value similar to the 95%–97% recovery of highly elastic sputter deposited FL-CN_x films. Given the dependence of the

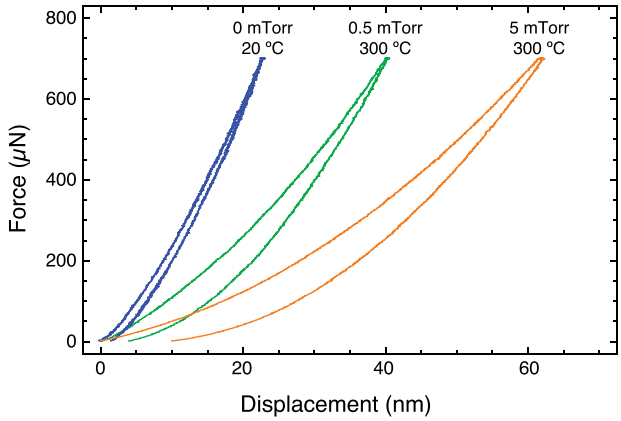

FIG. 10. Nanoindentation loading and unloading curves. The samples shown include the hard and highly elastic 0 mTorr, 20 °C sample and the softer and less elastic 5 mTorr, 300 °C sample.

recovery on the maximum applied load, however, and the relatively small maximum load used for these measurements, we examine trends within the dataset rather than making direct comparison with other results. The elastic recovery of the deposited films behaves in a more complex way than the film hardness as the deposition parameters are varied. Of the samples deposited at 0 or 0.5 mTorr N_2, the 20 °C and 300 °C samples are highly elastic, whereas there is a dip in the elastic recovery of the samples deposited at 175 °C. The reduced elastic recovery at 175 °C in the 0 and 0.5 mTorr samples may be related to the sp^3–sp^2 transition in this temperature range. No such dip in elastic recovery is observed in the samples deposited at 5 mTorr, where no sp^3–sp^2 transition occurs.

The FL films deposited at 175 °C are particularly notable, with hardnesses over 15 GPa. This hardness is sufficient for many industrial applications and since it can be achieved at a lower temperature by arc deposition than is possible with sputter deposition, a wider range of materials become potential substrates.

E. Consequences of nitrogen incorporation into arc-deposited C films

The effects of the addition of nitrogen to pulsed-arc deposited C films contrast with the results obtained when nitrogen is incorporated in C films during sputter deposition.

The incorporation of smaller amounts of nitrogen, up to 9 at. % at 0.5 mTorr, does not change the short-range order

TABLE I. Mechanical properties of C and CN_x films grown at different substrate temperatures and nitrogen pressures. For each sample, 10 indents were made and the error shown is the standard deviation.

T_s (°C)	$P(N_2)$ (mTorr)	Hardness (GPa)	Modulus (GPa)	% R (%)
20	0	48.8 ± 2.2	344 ± 5	95
	0.5	29.6 ± 0.4	249 ± 8	86
	5	13.3 ± 0.2	142 ± 3	68
175	0	26.6 ± 0.7	234 ± 3	81
	0.5	19.5 ± 0.4	182 ± 3	80
	5	10.4 ± 0.2	99 ± 2	76
300	0	21.8 ± 0.4	182 ± 5	94
	0.5	17.0 ± 0.4	145 ± 1	92
	5	8.3 ± 0.1	76 ± 1	84

of our films to an extent visible in the high-resolution TEM and ED data. This result is consistent with DC arc studies[3,6] showing that some nitrogen can be incorporated into ta-C films without disrupting their sp^3 bonding.

Deposition at 5 mTorr incorporates at least 15 at. % nitrogen into the film, affects the short-range order visible in TEM, and results in films with inferior mechanical properties. Sputter deposited FL-CN_x films, however, can incorporate nitrogen to 15 at. % and beyond while retaining their FL structure and mechanical properties. It is possible that the change in microstructure of our arc-deposited films at higher nitrogen fractions is not a direct consequence of the nitrogen incorporated in the film, but is instead a result of a change in the plasma conditions at higher N_2 pressure. The path length from the cathode to the substrate through the magnetic filter in the deposition system used is about 600 mm, and so is long in comparison with unfiltered deposition systems. This distance is much longer than the expected mean free path of the carbon ions in 5 mTorr N_2 (<100 mm, with the specific value dependent on the cross-sections used), suggesting that a substantial collision-induced reduction in the energy of the deposited species will result. This interpretation is consistent with the CN_x results of Hartmann *et al.*,[4] where the substrate was positioned facing away from the deposition flux, so that only scattered species were deposited. With this arrangement sp^3 hybridization of the films was reduced compared to films deposited at normal incidence.

IV. CONCLUSIONS

C and CN_x films were deposited using a pulsed cathodic arc source. The films produced fall into three classes. Deposition at a nitrogen pressure of 5 mTorr results in soft and under-dense films, while deposition at 20 °C with a nitrogen pressure of 0.5 mTorr or without nitrogen produces films with a majority of sp^3 hybridized carbon and an amorphous structure. A gradual transition between the sp^3-hybridized and the FL structure was found with increasing substrate temperature, in contrast with the sharp transition typically found for cathodic arc-deposited carbon films. At deposition temperatures of 175 °C and above, with either 0.5 mTorr nitrogen or without nitrogen, curved, FL structure is observed.

The effects of the addition of nitrogen to pulsed-arc deposited C films contrast with the results obtained when nitrogen is incorporated in C films during sputter deposition. The FL, cross-linked microstructure that nitrogen incorporation induces in sputtered CN_x films can be achieved in arc-deposited carbon films with no nitrogen, and at reduced substrate temperatures. High elastic recovery, one of the most desirable mechanical properties of FL-CN_x films, occurs in arc-deposited films both with and without nitrogen content, and both with and without FL structure.

ACKNOWLEDGMENTS

The research was funded by the European Research Council under the European Community Seventh Framework Program (FP7/2007-2013)/ERC Grant Agreement No. 258509 and the SSF frame program FUNCASE Functional Carbides and Advanced Surface Engineering. J. Rosen and L. Hultman acknowledge funding from the Knut and Alice Wallenberg Foundation. Zs. Czigány acknowledges support from the Bolyai Research Scholarship of the Hungarian Academy of Sciences. E. Broitman acknowledges the Swedish Government Strategic Research Area in Materials Science on Functional Materials at Linköping University (Faculty Grant SFO-Mat-LiU No. 2009-00971).

[1]L. Hultman, J. Neidhardt, N. Hellgren, H. Sjöström, and J.-E. Sundgren, MRS Bull. **28**, 194 (2003).
[2]J. Neidhardt and L. Hultman, J. Vac. Sci. Technol., A **25**, 633 (2007).
[3]C. A. Davis, Y. Yin, D. R. McKenzie, L. E. Hall, E. Kravtchinskaia, V. Keast, G. A. J. Amaratunga, and V. S. Veerasamy, J. Non-Cryst. Solids **170**, 46 (1994).
[4]J. Hartmann, P. Siemroth, B. Schultrich, and B. Rauschenbach, J. Vac. Sci. Technol., A **15**, 2983 (1997).
[5]A. Wienss, M. Neuhäuser, H. H. Schneider, G. Persch-Schuy, J. Windeln, T. Witke, and U. Hartmann, Diamond Relat. Mater. **10**, 1024 (2001).
[6]B. Kleinsorge, A. C. Ferrari, J. Robertson, and W. I. Milne, J. Appl. Phys. **88**, 1149 (2000).
[7]J. Koskinen, J.-P. Hirvonen, J. Levoska, and P. Torri, Diamond Relat. Mater. **5**, 669 (1996).
[8]A. A. Voevodin, J. G. Jones, T. C. Back, J. S. Zabinski, V. E. Strel'nitzki, and I. I. Aksenov, Surf. Coat. Technol. **197**, 116 (2005).
[9]I. Alexandrou, H.-J. Scheibe, C. J. Kiely, A. J. Papworth, G. A. J. Amaratunga, and B. Schultrich, Phys. Rev. B **60**, 10903 (1999).
[10]L. Ryves, M. M. M. Bilek, T. W. Oates, R. N. Tarrant, D. R. McKenzie, F. A. Burgmann, and D. G. McCulloch, Thin Solid Films **482**, 133 (2005).
[11]W. Oliver and G. Pharr, J. Mater. Res. **7**, 1564 (1992).
[12]E. Broitman, N. Hellgren, O. Wänstrand, M. Johansson, T. Berlind, H. Sjöström, J.-E. Sundgren, M. Larsson, and L. Hultman, Wear **248**, 55 (2001).
[13]Á. Barna, "Topographic Kinetics and Practice of Low Angle Ion Beam Thinning," in *Specimen preparation for transmission electron microscopy of materials III*, edited by R. Anderson, B. Tracy, and J. Bravman (Mater. Res. Soc. Symp. Proc., Pittsburgh, PA, 1991), Vol. 254, pp. 3–20.
[14]Z. Czigány, J. Neidhardt, I. F. Brunell, and L. Hultman, Ultramicroscopy **94**, 163 (2003).
[15]A. C. Ferrari, A. Libassi, B. K. Tanner, V. Stolojan, J. Yuan, L. M. Brown, S. E. Rodil, B. Kleinsorge, and J. Robertson, Phys. Rev. B **62**, 11089 (2000).
[16]N. Hellgren, M. P. Johansson, E. Broitman, L. Hultman, and J.-E. Sundgren, Phys. Rev. B **59**, 5162 (1999).
[17]H. Sjöström, I. Ivanov, M. Johansson, L. Hultman, J. E. Sundgren, S. V. Hainsworth, T. F. Page, and L. R. Wallenberg, Thin Solid Films **246**, 103 (1994).
[18]S. S. Todorov, D. Marton, K. J. Boyd, A. H. Al-Bayati, and J. W. Rabalais, J. Vac. Sci. Technol., A **12**, 3192 (1994).
[19]N. Hellgren, M. P. Johansson, E. Broitman, P. Sandström, L. Hultman, and J.-E. Sundgren, Thin Solid Films **382**, 146 (2001).
[20]J. Rosén, J. M. Schneider, and A. Anders, Appl. Phys. Lett. **89**, 141502 (2006).
[21]J. Rosén, E. Widenkvist, K. Larsson, U. Kreissig, S. Mráz, C. Martinez, D. Music, and J. M. Schneider, Appl. Phys. Lett. **88**, 191905 (2006).
[22]J. Rosén, K. Larsson, and J. M. Schneider, J. Phys.: Condens. Matter **17**, L137 (2005).
[23]D. R. McKenzie, Rep. Prog. Phys. **59**, 1611 (1996).
[24]Z. Czigány and L. Hultman, Ultramicroscopy **110**, 815 (2010).
[25]A. R. Merchant, D. G. McCulloch, D. R. McKenzie, Y. Yin, L. Hall, and E. G. Gerstner, J. Appl. Phys. **79**, 6914 (1996).
[26]S. D. Berger, D. R. McKenzie, and P. J. Martin, Philos. Mag. Lett. **57**, 285 (1988).
[27]H.-J. Scheibe, B. Schultrich, H. Ziegele, and P. Siemroth, IEEE Trans. Plasma Sci. **25**, 685 (1997).
[28]M. Chhowalla, A. C. Ferrari, J. Robertson, and G. A. J. Amaratunga, Appl. Phys. Lett. **76**, 1419 (2000).
[29]W. J. Gammon, O. Kraft, A. C. Reilly, and B. C. Holloway, Carbon **41**, 1917 (2003).

[30]N. Hellgren, J. Guo, Y. Luo, C. Såthe, A. Agui, S. Kashtanov, J. Nordgren, H. Ågren, and J.-E. Sundgren, Thin Solid Films **471**, 19 (2005).
[31]H. Sjöström, S. Stafström, M. Boman, and J.-E. Sundgren, Phys. Rev. Lett. **75**, 1336 (1995).
[32]J. Diaz, G. Paolicelli, S. Ferrer, and F. Comin, Phys. Rev. B **54**, 8064 (1996).
[33]M. Chhowalla, J. Robertson, C. W. Chen, S. R. P. Silva, C. A. Davis, G. A. J. Amaratunga, and W. I. Milne, J. Appl. Phys. **81**, 139 (1997).
[34]M. B. Taylor, D. W. M. Lau, J. G. Partridge, D. G. McCulloch, N. A. Marks, E. H. T. Teo, and D. R. McKenzie, J. Phys.: Condens. Matter **21**, 225003 (2009).
[35]J. Rosén, A. Anders, S. Mráz, and J. M. Schneider, J. Appl. Phys. **97**, 103306 (2005).
[36]N. Hellgren, M. P. Johansson, E. Broitman, L. Hultman, and J.-E. Sundgren, Appl. Phys. Lett. **78**, 2703 (2001).
[37]D. W. M. Lau, D. G. McCulloch, M. B. Taylor, J. G. Partridge, D. R. McKenzie, N. A. Marks, E. H. T. Teo, and B. K. Tay, Phys. Rev. Lett. **100**, 176101 (2008).